Electroanatomical voltage mapping with contact force sensing for diagnosis of arrhythmogenic right ventricular cardiomyopathy

Saguner, A M ; Lunk, D ; Mohsen, Mona ; Knecht, Sven ; Akdis, Deniz ; Costa, Sarah ; Gasperetti, Alessio ; Duru, Firat ; Rossi, V A ; Brunckhorst, C B

Abstract: Background Three-dimensional electroanatomical mapping (EAM) can be helpful to diagnose arrhythmogenic right ventricular cardiomyopathy (ARVC). Yet, previous studies utilizing EAM have not systematically used contact-force sensing catheters (CFSC) to characterize the substrate in ARVC, which is the current gold standard to assure adequate tissue contact. Objective To investigate reference values for endocardial right ventricular (RV) EAM as well as substrate characterization in patients with ARVC by using CFSC. Methods Endocardial RV EAM during sinus rhythm was performed with CFSC in 12 patients with definite ARVC and 5 matched controls without structural heart disease. A subanalysis for the RV outflow tract (RVOT), septum, free-wall, subtricuspid region, and apex was performed. Endocardial bipolar and unipolar voltage amplitudes (BVA, UVA), signal characteristics and duration as well as the impact of catheter orientation on endocardial signals were also investigated. Results ARVC patients showed lower BVA vs. controls ($p = 0.018$), particularly in the subtricuspid region (1.4, IQR:0.5–3.1 vs. 3.8, IQR:2.5-5 mV, $p = 0.037$) and RV apex (2.5, IQR:1.5–4 vs. 4.3,IQR:2.9–6.1 mV, $p = 0.019$). BVA in all RV regions yielded a high sensitivity and specificity for ARVC diagnosis (AUC 59–78%, $p < 0.05$ for all), with the highest performance for the subtricuspid region (AUC 78%, 95% CI:0.75–0.81, $p < 0.001$, negative predictive value 100%). A positive correlation between BVA and an orthogonal catheter orientation (46°-90°:$r = 0.106$, $p < 0.001$), and a negative correlation between BVA and EGM duration ($r = -0.370$, $p < 0.001$) was found. Conclusions EAM using CFSC validates previous bipolar cut-off values for normal endocardial RV voltage amplitudes. RV voltages are generally lower in ARVC as compared to controls, with the subtricuspid area being commonly affected and having the highest discriminatory power to differentiate between ARVC and healthy controls. Therefore, EAM using CFSC constitutes a promising tool for diagnosis of ARVC.

DOI: https://doi.org/10.1016/j.ijcard.2023.131289

diagnosis of arrhythmogenic right ventricular cardiomyopathy. International Journal of Cardiology, 392:131289. DOI: https://doi.org/10.1016/j.ijcard.2023.131289

International Journal of Cardiology 392 (2023) 131289

Contents lists available at ScienceDirect

International Journal of Cardiology

journal homepage: www.elsevier.com/locate/ijcard

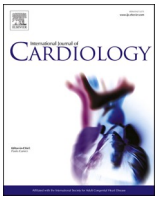

Electroanatomical voltage mapping with contact force sensing for diagnosis of arrhythmogenic right ventricular cardiomyopathy

A.M. Saguner [a,b,*,1], D. Lunk [a,1], M. Mohsen [a,c], Sven Knecht [d], Deniz Akdis [a], S. Costa [a], A. Gasperetti [a,e], F. Duru [a,b], V.A. Rossi [a,2], C.B. Brunckhorst [a,2]

[a] Arrhythmia Division, Department of Cardiology, University Heart Center Zurich, University Hospital Zurich, Zurich, Switzerland
[b] Center for Translational and Experimental Cardiology (CTEC), Department of Cardiology, Zurich University Hospital, University of Zurich, 8952 Schlieren, Switzerland
[c] Department of Cardiology, Qatar Heart Hospital 7GR5+RW4, Doha, Qatar
[d] Cardiology, University Hospital Basel, University of Basel, Basel, Switzerland
[e] Division of Cardiology, Department of Medicine, Johns Hopkins Hospital, Carnegie 568D, 600 N. Wolfe St., Baltimore, MD 21287, USA

ARTICLE INFO

Keywords:
Electroanatomical voltage mapping
Arrhythmogenic right ventricular cardiomyopathy
Arrhythmogenic right ventricular dysplasia
Contact force

ABSTRACT

Background: Three-dimensional electroanatomical mapping (EAM) can be helpful to diagnose arrhythmogenic right ventricular cardiomyopathy (ARVC). Yet, previous studies utilizing EAM have not systematically used contact-force sensing catheters (CFSC) to characterize the substrate in ARVC, which is the current gold standard to assure adequate tissue contact.

Objective: To investigate reference values for endocardial right ventricular (RV) EAM as well as substrate characterization in patients with ARVC by using CFSC.

Methods: Endocardial RV EAM during sinus rhythm was performed with CFSC in 12 patients with definite ARVC and 5 matched controls without structural heart disease. A subanalysis for the RV outflow tract (RVOT), septum, free-wall, subtricuspid region, and apex was performed. Endocardial bipolar and unipolar voltage amplitudes (BVA, UVA), signal characteristics and duration as well as the impact of catheter orientation on endocardial signals were also investigated.

Results: ARVC patients showed lower BVA vs. controls ($p = 0.018$), particularly in the subtricuspid region (1.4, IQR:0.5–3.1 vs. 3.8, IQR:2.5-5 mV, $p = 0.037$) and RV apex (2.5, IQR:1.5–4 vs. 4.3,IQR:2.9–6.1 mV, $p = 0.019$). BVA in all RV regions yielded a high sensitivity and specificity for ARVC diagnosis (AUC 59–78%, $p < 0.05$ for all), with the highest performance for the subtricuspid region (AUC 78%, 95% CI:0.75–0.81, $p < 0.001$, negative predictive value 100%). A positive correlation between BVA and an orthogonal catheter orientation (46°-90°:$r = 0.106$, $p < 0.001$), and a negative correlation between BVA and EGM duration ($r = -0.370$, p < 0.001) was found.

Conclusions: EAM using CFSC validates previous bipolar cut-off values for normal endocardial RV voltage amplitudes. RV voltages are generally lower in ARVC as compared to controls, with the subtricuspid area being commonly affected and having the highest discriminatory power to differentiate between ARVC and healthy controls. Therefore, EAM using CFSC constitutes a promising tool for diagnosis of ARVC.

1. Introduction

Arrhythmogenic right ventricular cardiomyopathy (ARVC) is an inherited cardiomyopathy mainly caused by desmosomal abnormalities leading to fibro-fatty replacement predominantly of the right ventricular (RV) myocardium. These changes usually begin in the subepicardial RV layers and progress towards the endocardium over time, potentially leading to malignant ventricular arrhythmias and sudden cardiac death (SCD), particularly in athletes [1,2]. The diagnosis of ARVC relies upon the 2010 Task Force Criteria, which can fail to detect early forms of the disease, when the phenotype is not yet fully present, but the risk of SCD due to VF is particularly high [3]. Furthermore, there is substantial

* Corresponding author at: Arrhythmia Division, Department of Cardiology, University Heart Center Zurich, Rämistrasse 100, 8091 Zürich, Switzerland.
E-mail address: ardansaguner@yahoo.de (A.M. Saguner).
[1] Shared first authorship.
[2] Shared last authorship.

https://doi.org/10.1016/j.ijcard.2023.131289
Received 21 April 2023; Received in revised form 17 August 2023; Accepted 20 August 2023
Available online 22 August 2023

overlap between ARVC and other cardiopathies with RV involvement such as myocarditis, Brugada syndrome, cardiac sarcoidosis and the athlete's heart, which can render correct diagnosis and management difficult [4,5].

Three-dimensional (3D) electroanatomical mapping (EAM) uses biologically inert low-intensity magnetic field energy to determine the location of sensor-tipped diagnostic catheter electrodes in the heart chambers. Areas with low voltage local electrograms (LVA) in the RV have been described in ARVC and indicate the presence of abnormal RV tissue, which can be picked up by EAM [6]. The presence of fractionated electrograms (EGMs) of low voltage and prolonged duration may help to distinguish ARVC from healthy probands, the athlete's heart and other RV abnormalities mimicking ARVC [7,8]. EAM is not yet considered in the 2010 revised Task Force due to its invasive nature, technical challenges and, so far, small-scale studies having been performed mostly in patients with advanced forms of the disease with associated limitations in sensitivity and specificity [9,10]. With regard to these aspects, EAM could represent an important additional tool to facilitate correct and early diagnosis of ARVC. However, previous studies using EAM in ARVC have not systematically assessed the amount and distribution of LVA by contact-force sensing technology (CFST) – the current gold standard to assure adequate tissue contact -, and their statistical analyses did not take differences in the electrophysiological properties of each individual patient into account [11,12].

Therefore, the aim of this prospective endocardial EAM study was to 1) determine cut-off values to differentiate between diseased RV myocardium and healthy controls using CFST 2) delineate the regional distribution and signal characteristics of LVA as a surrogate parameter of fibro-fatty infiltration in patients with ARVC. 3) assess the impact of contact force and catheter angulation on signal characteristics.

2. Methods

2.1. Patient cohort

In this prospective, single-center study 12 consecutive patients with definite ARVC according to the 2010 Task Force Criteria and 5 controls without structural heart disease referred for electrophysiological study due to supraventricular tachycardia or palpitations of unknown origin undergoing 3D endocardial EAM (Biosense Webster, CARTO3, Diamond Bar, CA) of the RV using a CF sensing catheter (Thermocool Smarttouch, Biosense Webster) were included. Genetic testing for ARVC-associated genetic variants was performed in all ARVC patients. Participants signed an informed consent form for participation in this study, which was approved by the Zurich Cantonal Ethical committee (approval numbers: KEK-ZH-Nr. 2011–0208 and PB_2016–02109).

2.2. 3D EAM and analysis

In brief, after right-sided femoral venous puncture, the CF sensing catheter was inserted into the RV under fluoroscopic guidance via a long sheath (Agilis or SL-1, Abbott, Chicago, IL). The EAM procedure in all patients was performed during sinus rhythm. Points were taken with a homogenous distribution throughout the different RV segments (fill threshold >15 mm) with a higher density in LVA. Electrograms (EGMs) were filtered at 30 to 500 Hz (bipolar) and 1 to 240 Hz (unipolar). EGMs were displayed at the same gain (0.2 mV/cm for bipolar voltage (BV) and 1.0 mV/cm for unipolar voltage (UV)) and sweep speed (400 mm/s) on CARTO. Only points with adequate tissue contact (mean force ≥4 g measured by the CF sensing catheter) were selected based on review of all EGMs. Points taken during or after ablation, ectopic beats, floating points, and points tagged as location only were excluded. The unipolar and bipolar peak-to-peak voltage amplitudes (UVA and BVA, respectively) were measured automatically. LVA as defined by voltage cut-off points generated by our study had to cover an area of ≥1cm^2 including at least 3 adjacent points [6]. Signal duration was defined as the distance between the earliest sharp peak deflection and the latest sharp peak deflection, as previously described [13]. Potentials with a rounded component with or without separation from the sharp component were considered to represent far-field remote electrical activity and were not included in the duration measurement. Fragmentation was defined as a multicomponent (>2 deflections) signal. The degree of fragmentation was quantified by the number of positive electrogram deflections recorded at a gain of 0.2 mV/cm at 400 mm/s [14,15]. Late potentials were defined as local ventricular potentials occurring after the terminal portion of the surface QRS complex being distinct and separated by an isoelectric line from the first ventricular component [16,17]. To assess the impact of catheter orientation on EGM characteristics, we structured the catheter contact angles into the following categories: a) 0°-30° (e.g. 0° = electrode parallel to the endocardial surface) b) 31°-45 °c) 46°-90°. Betablockers/antiarrhythmic drugs were stopped 5 half-lives prior to EAM, whereas amiodarone was stopped two weeks prior to the study.

2.3. Unipolar and bipolar voltage distribution per RV segment

To analyze regional differences in UV and BV, the RV was divided into 5 regions: RV outflow tract (RVOT), septum, anterior free wall, subtricuspid region and apex as previously suggested [17]. Points were manually selected for analysis and distributed to each region by two independent observers.

2.4. Statistical analysis

Categorical variables are expressed as number and percentage and compared using the Chi-square test or Fisher exact test. Continuous variables are expressed as mean +/− SD or median (interquartile range) and compared between groups using Student's *t*-test or Mann-Whitney *U* test. Paired samples were compared using Wilcoxon signed rank test or McNemar test. Correlation analyses were assessed with Pearson test, with the measure of correlation reported as the Pearson product-moment correlation coefficient (r) and corresponding *P* values. A repeated measurements ANOVA was performed on a per-patient basis to assess for individual differences in the electrophysiologic properties (e.g. EGM amplitude, duration) in the RV segments. A mixed-effect repeated measures ANOVA was performed to compare the mean differences between bipolar voltage values in ARVC patients as compared with controls. The Mauchly's test for sphericity assumption was performed for this comparison. In the control group, normal endocardial amplitudes were defined as a signal amplitude exceeding by 95% all electrogram signals for the RV for both bipolar and unipolar measurements. To individuate the cut-off values between healthy and diseased myocardium, an average of all 5th percentile values per patient was determined. Receiver-Operating-Characteristic (ROC) curves were calculated to assess the area under the curve (AUC), sensitivity and specificity of different LVA cut-off values using Youden's Index. A p value <0.05 was considered significant. All statistical analyses were performed with SPSS software (v25, SPSS Inc., USA).

3. Results

3.1. Study population

Twelve patients with a definite diagnosis of ARVC according to the 2010 Task Force Criteria and 5 gender- and age-matched subjects without structural heart disease as controls were included. Baseline characteristics are summarized in Table 1. None of the control subjects fulfilled any criterion for ARVC diagnosis and did not display any signs of RV structural and electrical changes.

3.2. Bipolar and unipolar voltage values

A median of 227 (120–364) reference points per patient were

Table 1
Baseline characteristics.

	ARVC $N = 12$	Controls $N = 5$	P-value
Age (mean +/− SD)	40.7 (13.2)	43.4 (14)	0.714
Male	9 (75)	3 (60)	0.280
LVEF %	51.8 (10.4)	56.8 (5.6)	0.328
RV fac %	28.4 (9.1)	40.3 (9.5)	0.042
ARVC 2010 Task force criteria (major+minor criteria)	3 (2–3.3)	0	0.002
Arrhythmic syncope	4 (33)	0	0.261
Cardiac arrest	0	0	1
ICD	11 (92)	0	0.001
Betablocker	7 (58)	2 (40)	0.620
Amiodarone	1 (8)	0	1
(Likely)pathogenic genetic variants	N = 5 (42%)	NA	
PKP-2	$N = 2$		
DSG-2	N = 2		
DSP	N = 1		
Gene elusive	$N = 7$		

Abbreviations: ARVC, arrhythmogenic right ventricular cardiomyopathy; ICD, implantable cardioverter-defibrillator; DSG2, desmoglein 2; DSP, desmoplakin; LV, left ventricular; LVEF, left ventricular ejection fraction; PKP2, plakophilin-2; RV fac, right ventricular fractional area change determined by transthoracic echocardiography.
Values are mean (± standard deviation), median (interquartile range), or n (%) as appropriate.

analyzed (Table 2). The median contact force was 10 g (6–17) in the healthy and 11 g (6–17) in the ARVC population ($p = 0.447$). The cut-off values for endocardial bipolar and unipolar voltage for the RV in total and each of the 5 segments based on our controls are provided in Table 2. Derived from the controls, our study determined ≥1.8 mV as the optimal cut-off for normal endocardial RV bipolar voltages, and ≥ 3.4 mV for normal unipolar voltages. The bipolar cut-off values derived from healthy controls were similar between the 5 RV segments, whereas the unipolar cut-off values were higher in the RV septum and RV apex as compared to the other RV segments, and lowest in the RVOT (Tables 2 and 3).

A comparison between ARVC patients and controls using repeated measures ANOVA revealed significantly lower mean bipolar endocardial voltages in patients with ARVC as compared to controls (Table 2; between-subjects effect: F 7.080, $p = 0.018$). The Mauchly's test for sphericity assumption revealed no violation ($\chi^2(9) = 13.6$, $p = 0.141$). No significant differences were observed for unipolar voltages.

For bipolar voltages, the lowest values in patients with ARVC were found in the subtricuspid area followed by the RVOT, the RV apex, RV free wall and RV septum. For unipolar voltages, the lowest values in patients with ARVC were also found in the subtricuspid area, followed by the RVOT, the RV apex, the RV free wall and the RV septum. In the control population, highest bipolar voltages were found in the apical area, followed by the septum, the subtricuspid area, the RV free wall and the RVOT, and highest unipolar voltages were found in the septum followed by the RV apex, the RVOT, the subtricuspid area and the RV free wall, respectively (Table 2). ARVC patients presented significantly lower bipolar voltages in the subtricuspid region ($p = 0.037$) and in the RV apex ($p = 0.019$) as compared to controls (Table 2).

According to ROC curves, endocardial bipolar voltage values in the RVOT, subtricuspid region, RV free wall, RV septum and RV apex all yielded a high sensitivity and specificity for diseased myocardium in patients with ARVC (AUC 0.59 to 0.78, $p < 0.05$ for all), with the highest performance for the subtricuspid region (AUC 0.78, 95% CI 0.75–0.81, $p < 0.001$). A bipolar voltage value <1.6 mV in the subtricuspid region yielded a sensitivity of 96% and a specificity of 54% for ARVC diagnosis (Fig. 1). Similar findings were found for unipolar voltages in the subtricuspid region (AUC 0.83, 95% CI 0.80–0.86, p < 0.001), with a voltage value <3.2 mV yielding a sensitivity of 95% and a specificity of 48% for ARVC diagnosis (Table 3). The proposed cut-offs for bipolar voltages yielded a high negative predictive value for all RV regions. The subtricuspid region presented also with the highest positive predictive values (Table 3). Voltage amplitudes for all RV regions in all the 12 ARVC patients are presented in supplementary table 1.

3.3. Signal duration, EGM fragmentation and late potentials

All ARVC patients displayed EGM fragmentation and all but one patient late potentials [18]. Electrogram signal duration was higher in ARVC patients as compared to controls (mean 22.5 ± 0.4 ms vs 5.9 ± 0.2 ms, median 16 ms (IQR:10–28) vs. 13 ms (IQR:10–18), $p < 0.001$). When analyzed separately for each RV segment, the longest signal duration was found in the subtricuspid region (see Table 2). The most frequent location for fragmentation was the subtricuspid area (6% of all measurements in this segment), followed by the RVOT (5%), RV septum (3%), and RV apex (1%), whereas no fragmentation was registered in the RV free wall. The most frequent locations for late potentials were the subtricuspid area and RV apex (both 26%, respectively), followed by the

Table 2
Comparison between bipolar and unipolar voltage values in ARVC patients and controls.

	ARVC N = 12			Controls N = 5				
	Bipolar voltage (mV)	5–95%	Signal duration (ms)	Bipolar voltage (mV)	5–95%	Signal duration (ms)	*p*-values for voltage	p-values for signal duration
RVOT	2.3 (1.3–3.5)	0.24–6.9	15 (9–25)	3.6 (2.7–4.5)	1.9–7.9	13 (10–17)	0.130	**0.019**
Subtricuspid region	1.4 (0.5–3.1)	0.1–6.5	20 (11–36)	3.8 (2.5–5)	1.6–8.8	14 (11–17)	**0.037**	**<0.001**
RV free wall	3 (2–4.3)	1–7	14 (10−22)	3.7 (2.8–5)	1.9–7.5	14 (11–19)	0.574	0.624
RV apex	2.5 (1.5–4)	0.3–7.1	15 (9–27)	4.3 (2.9–6.1)	1.8–8.9	13 (9–17)	**0.019**	**0.001**
RV septum	3.8 (2.2–6.3)	0.6–11.7	16 (11−32)	4.6 (3.2–7)	1.7–19.3	11 (9–15)	0.721	**<0.001**
Total	2.5 (1.2–4.1)	0.2–7.9	16 (10–28)	3.8 (2.7–5.4)	1.8–9	13 (10–18)	**0.018**	**<0.001**

	Unipolar voltage (mV)	5–95%	Unipolar voltage (mV)	5–95%	p-values for voltage
RVOT	4.3 (3–6.3)	1.8–9.7	6 (4.6–8.8)	2.7–13.2	0.442
Subtricuspid region	3.4 (1.9–5.2)	1.1–9.8	7.1 (5.5–8.7)	3.2–11.8	0.160
RV free wall	5.4 (3.9–8.5)	2.1–13.1	6.6 (5.6–8.7)	3.7–12.4	0.234
RV apex	4.9 (3.2–6.6)	1.6–10.1	7.8 (6–9.8)	4–11.6	**0.006**
RV septum	9 (5.2–11.7)	2.8–15.3	9.7 (7.6–11.4)	5–15.1	0.721
Total	5 (3.75–7)	2–8.9	7 (7–9.4)	3.4–12.4	0.283

Table 3
ROC curves, sensitivity/specificity and positive/negative predictive values for cut-off values for bipolar and unipolar voltages based on controls.

RV area	Bipolar voltage (mV)						
	Cut-off	AUC (95% CI)	Sensitivity	Specificity	PPV	NPV	p-value
RVOT	1.9	72% (0.69–0.76)	95%	40%	42%	100%	<0.001
Subtricuspid region	1.6	78% (0.75–0.81)	96%	54%	58%	100%	<0.001
RV free wall	1.9	62% (0.57–0.67)	96%	20%	17%	100%	<0.001
RV apex	1.8	74% (0.69–0.78)	96%	35%	25%	100%	<0.001
RV septum	1.7	59% (0.52–0.66)	96%	15%	0	100%	0.015
Total	1.8	70% (0.68–0.73)	95%	35%	28%	100%	<0.001

RV area	Unipolar voltage (mV)						
	Cut-off	AUC (95% CI)	Sensitivity	Specificity	PPV	NPV	p-value
RVOT	2.7	69% (0.64–0.73)	70%	19%	17%	100%	<0.001
Subtricuspid region	3.2	83% (0.79–0.86)	95%	48%	33%	80%	<0.001
RV free wall	3.7	61% (0.56–0.66)	96%	20%	17%	60%	<0.001
RV apex	4	80% (0.76–0.84)	94%	37%	17%	100%	<0.001
RV septum	5	56% (0.50–0.63)	95%	20%	25%	100%	0.091
Total	3.4	72% (0.70–0.74)	95%	29%	22%	90%	<0.001

Receiving Operator Curves (ROC), sensitivity, specificity, positive predictive value (PPV), and negative predictive value (NPV) for bipolar and unipolar values are presented for each RV region. Abbreviations: AUC, area under the curve; CI, confidence interval; RV, right ventricular; RVOT, right ventricular outflow tract.

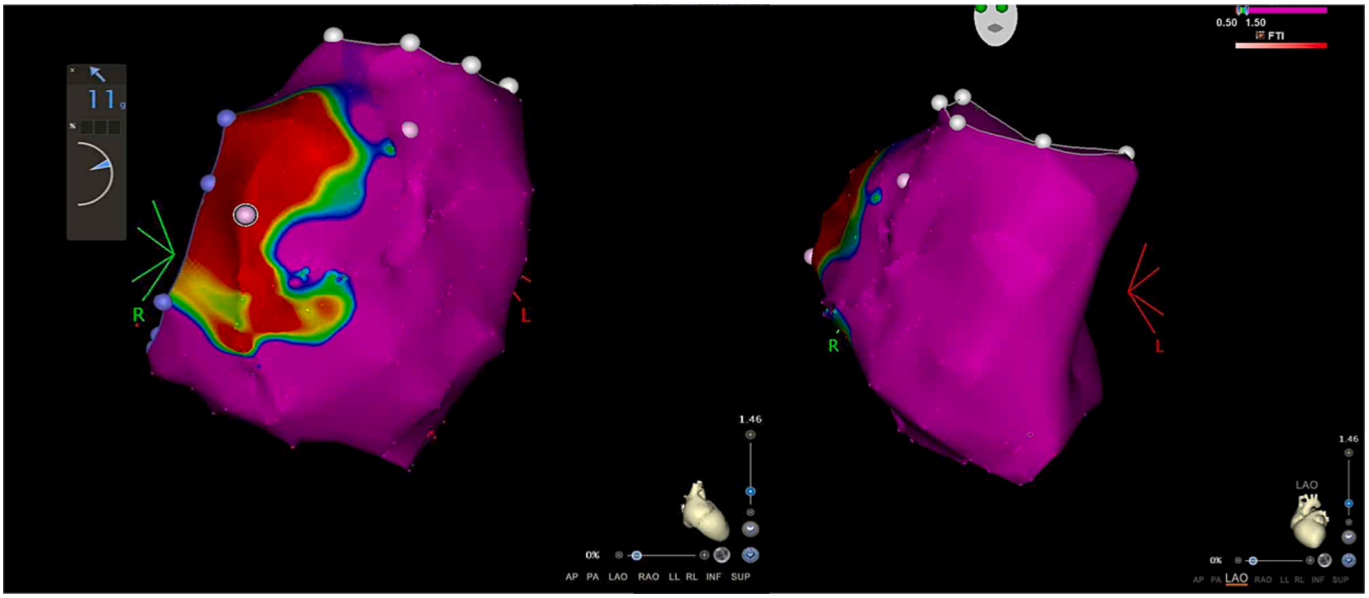

Fig. 1. CARTO mapping in RAO (left) and LAO (right). Adequate tissue contact was verified by a contact force ≥4G during endocardial EAM of the RV, and confirmed the typical C-type scar in the subtricuspid region (RAO projection, on the left), whereas the RV apex and septum showed normal values in patients with ARVC and less advanced disease stage (LAO projection, on the right).

RVOT region (19%), the RV free wall and RV septum (both 11%, respectively). None of the controls displayed EGM fragmentation nor late potentials.

3.4. Catheter orientation

We noted a positive correlation between bipolar voltage values and a catheter orientation between 46° and orthogonal 90° ($r = 0.106$), whereas no relevant correlation between lower angles of catheter orientation and bipolar voltage values were observed (0.-30°, $r = -0.067$). Between bipolar voltage values and electrogram duration ($r = -0.370$, $p < 0.001$) a negative correlation was found. Similarly, unipolar voltage values negatively correlated with electrogram duration ($r = -0.55$). Unipolar voltage values did not correlate with catheter orientation ($r = 0.001$).

3.5. Procedural safety

The EAM procedure using the force-sensing catheter was safe. No periprocedural complication related to endocardial RV voltage mapping occurred. One patient developed pericardial tamponade that was treated by successful pericardiocentesis following endomyocardial biopsy from the RV at the end of the procedure, which was deemed unrelated to the EAM procedure.

4. Discussion

The diagnosis of ARVC remains challenging. The 2010 revised Task Force Criteria emphasize that current criteria are “not perfect”, still lead to underrecognition of the disease and highlight that future improvements in diagnostic tools are urgently needed [3,10]. The 2020 Padua Criteria have recently been published in order to improve the diagnostic

process in patients with arrhythmogenic cardiomyopathy, but larger validation studies are still pending and they also do not include EAM [9]. In this study, we showed that endocardial 3D EAM with CFSC - which is the current gold standard to ensure adequate tissue contact - represents a useful method to detect the pathologic substrate of ARVC, and to differentiate affected myocardial areas from unaffected ones. In our study we report the following main findings:

1. EAM using CFSC validated previous bipolar cut-off values for normal endocardial RV voltage amplitudes, which were previously established without CFSC.
2. ARVC patients displayed significantly lower mean bipolar endocardial RV voltages as compared to controls.
3. We found that the subtricuspid region is commonly affected in ARVC and has the best discriminatory power to differentiate between patients with ARVC and healthy subjects.
4. Bipolar voltage values above our proposed cut-off values have a high negative predictive value for a diagnosis of ARVC.

4.1. Reference values for endocardial RV voltage mapping

Reference values for endocardial right ventricular EAM as well as substrate characterization in patients with ARVC using CFSC have not been systematically investigated, yet. Up to now, reference values for normal bipolar and unipolar voltages have been derived without CFSC using older technologies and mostly with a low resolution with <100 points obtained from the RV. Moreover, previous findings have yielded somewhat differing results for reference values for normal endocardial bipolar RV voltage (between >1.2 and > 1.5 mV), whereas scars were arbitrarily defined as LVA <0.5 mV based on a limited sample size of patients using mapping catheters without CFSC [13]. In one of the first studies investigating EAM in ARVC patients, Boulos et al. analyzed 90 ± 16 endocardial RV points in 5 different RV sites under fluoroscopic guidance and compared the results of ARVC patients with controls with RV outflow tract tachycardia and no structural heart disease [6,7]. ARVC patients were characterized by significantly lower unipolar and bipolar voltage amplitudes in affected areas as compared to the average voltage values in not affected myocardium of the same patients [6]. Indeed, Boulos and colleagues reported lower mean bipolar and unipolar endocardial voltages in ARVC patients as compared to controls (2.7 ± 2.2 vs. 4.9 ± 2.5 mV, $p < 0{,}001$ and 4 ± 2.3 vs. 6.9 ± 3.6 mV, $p < 0.001$, respectively) [6]. Similarly, data from another study comparing ARVC patients with controls without structural heart disease proposed an unipolar voltage cut-off value of <5.5 mV in the RV [19]. These findings support our data, which consistently showed lower endocardial RV voltages in ARVC as compared to healthy controls both on average and in the 5 different RV sites analyzed separately. However, these previous studies were affected by statistical limitations, such as the use of one-way ANOVA instead of repeated measurements ANOVA, namely comparison of the means from all patients instead of comparison of the means per patient [6,7]. To overcome the above-mentioned statistical limitations, we performed repeated measurements ANOVA and defined RV reference values by using a threshold ≥5th percentile of measurements in controls, thus providing reliable cut-off values

Derived from our controls using CFSC, our study determined ≥1.8 mV as the optimal cut-off for normal bipolar voltages, and ≥ 3.4 mV for normal unipolar voltages. The bipolar cut-off values for healthy RV myocardium were similar between the 5 RV segments, whereas the unipolar cut-off values were higher in the RV septum and RV apex as compared to the other RV segments, and lowest in the RVOT (Table 2). This reflects that the RV septum is the thickest, whereas the RVOT, particularly towards the free wall, is one of the thinnest RV structures [20]. Our findings are similar to previous literature derived from studies not using CFSC, particularly for bipolar voltages (≥1.8 mV in our study vs. ≥1.5 mV recommended in daily clinical practice) [7,21]. However, cut-off values for normal unipolar voltages were lower as values recently suggested without CFSC (≥3.4 mV in our study vs. ≥5.5 mV recommended in daily clinical practice). The reason for this finding remains not fully clear, but may be related to differences in assuring adequate tissue contact with CFSC vs. non-CFSCs as well as our defined minimum contact force of 4G.

In general, ARVC patients presented with lower endocardial RV voltages as a sign of structural myocardial disease as compared to healthy controls, particularly in the subtricuspid area and RV apex. The robustness of cut-off values is critical in clinical practice as it may allow improved detection of patients who are more likely to be affected by ARVC and other RV structural diseases. Based on our findings, CFSC can facilitate the detection of diseased RV regions, particularly in the subtricuspid region for ARVC, and may improve the yield of endomyocardial biopsy as previously shown by our group for cardiac sarcoid and other groups for ARVC [8,22–24]. We were not able to show significantly lower endocardial bipolar voltages in the RVOT, RV free wall and septum of patients with ARVC vs. healthy controls. Similarly, no significant mean differences for unipolar endocardial RV voltages in ARVC vs. healthy controls were observed. This somewhat differs from previous literature and may be related to the different statistical (repeated measurements ANOVA) and mapping methods used in our study, as well as a rather low sample size of patients [6,7]. Of interest, electrogram signal duration was significantly longer in patients with ARVC as compared to controls, not only for the total RV, but also most RV segments except the RV free wall. Therefore, besides voltage amplitudes, signal duration may be used to diagnose ARVC and other RV cardiopathies in the future. Since manual measurement of signal duration poses challenges in daily clinical practice, automated algorithms may facilitate this process [25]. Of note, RV endocardial EAM might be a helpful tool in differentiating ARVC from the athlete's heart – a phenocopy, which shares with ARVC many morphological features, particularly dilatation of the right-sided heart chambers, but without fibro-fatty infiltration that can be potentially picked up by EAM [26,27].

4.2. ARVC – A subtricuspid disease

The observation that fibro-fatty infiltration often starts in the subtricuspid area, extending to the RVOT and later to the RV apex, but often sparing the septum, was well reproduced by our study [28]. The finding of LVA in these RV locations is supported by morphological findings on endomyocardial biopsy showing significantly reduced myocardial fibers replaced by fibrous and/or fatty tissue in patients with ARVC [24]. Accordingly, abnormal RV EAMs have been associated to RV wall motion abnormalities on imaging and to myocyte loss and fibrofatty replacement in endomyocardial biopsies of ARVC patients [22].

We found that the subtricuspid RV area is commonly affected in classical ARVC, even at earlier disease stages, which is in line with the morphologic findings of the early stages of ARVC (RV subtricuspid aneurysms) [3]. The subtricuspid area showed the highest AUC for differentiating ARVC from healthy controls, not only for bipolar voltages, but also unipolar voltages with a high sensitivity. Moreover, the subtricuspid area was the RV region displaying the longest electrogram duration, highest percentage of fragmentation and late potentials as compared to other RV segments in patients with ARVC. As such, we could confirm - with the use of CFSC - that the typical substrate consisting of fibro-fatty infiltration is predominantly located in a "C-type scar pattern" involving the peritricuspid area (Figs. 1 and 2), whereas the RV apex is involved at more advanced disease stages [28,29]. This finding provides new evidence to the natural course of ARVC. Indeed, previous studies performing analyses with bipolar endocardial RV voltage maps without CFSC – which is less sensitive in displaying the early pathologic process of fibro-fatty infiltration as compared with epicardial voltage maps – failed to show this typical "C-shape pattern" of disease involvement in up to 43% of the performed endocardial bipolar maps [28]. This ARVC-typical distribution of substrate/LVA in the RV

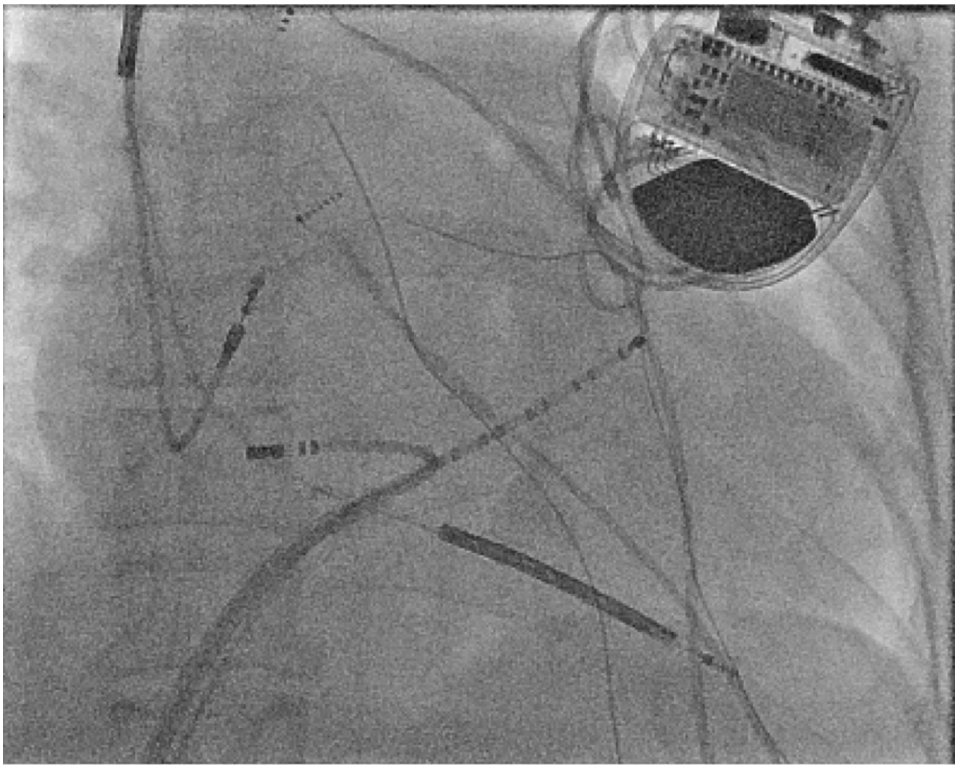

Fig. 2. Endocardial EAM mapping by using a long sheath and looping the mapping catheter within the RV to perpendicularly reach the peritricuspid region.

can sometimes only be visualized by unipolar endocardial or epicardial voltage mapping, which better reflects that the disease typically starts in the subepicardial RV layers.

On the contrary, septal biopsy did not provide any added diagnostic value in previous studies, thus confirming our findings, which showed no significant differences in voltages in the septal area in ARVC as compared to healthy controls [24]. Of interest, the basal septal involvement is frequently seen in cardiac sarcoidosis, whereas this is a rare finding in ARVC [30].

In line with more recent findings, showing that the RV apex is not affected at earlier disease stages, we found a rather low rate of RV apical involvement in patients with definite ARVC [29]. Therefore, the measurement of RV apical voltage may be useful to differentiate ARVC from cardiac sarcoidosis, which frequently involves the septum and RV apex [5,30].

4.3. The impact of catheter angulation on voltage and signal duration

The intracardiac electrogram depends on the myocardial characteristics (the source of the electrical signal), on the catheter configuration and orientation. Tissue contact, reflecting the distance of the electrode to the electric source with the catheter tip was verified in previous studies using catheters without CFSC by a fluoroscopic stable catheter position and by eliminating points in which: 1) the values of the local stability variables were greater than predetermined values (end-diastolic location stability >3 mm and local activation time stability >3 ms); and 2) extreme pressure was applied, as identified by significant ST segment elevation on the unipolar recording [6,13,21,22,31]. Nevertheless, it is sometimes very difficult to distinguish LVA resulting from poor tissue contact with true low voltage resulting from fibro-fatty infiltration with conventional catheters [6,13,21,22,31]. This limitation is addressed by the continuous measurement and visualization of the resulting contact force using the CFSC. In addition, we showed a weak, but positive correlation between bipolar voltages and an orthogonal catheter orientation (between 46° and 90°). Furthermore, we observed a negative correlation between bipolar voltage values and electrogram duration.

Since the bipolar voltage electrogram is determined by the temporal difference of the unipolar electrograms of the electrode pair, the orientation of these two electrodes with regards to the propagation wave front is of high importance [32]. As shown in a numerical simulation, the ring electrode unipolar voltage but not the tip unipolar voltage does correlate with catheter angulation [33]. This results in an orientation dependent amplitude characteristics. With a perpendicular catheter orientation with a symmetric unipolar signal on both electrodes, however, the dependency on the wave front propagation can be eliminated. This might explain the observed positive correlation between catheter orientation and BVA only for large catheter angulations >45°.

Catheter orientation is particularly important when mapping the perivalvular region of the tricuspid valve, as appropriate catheter contact with the myocardium in this region is difficult. However, optimal contact forces for ventricular mapping have not been validated, yet. In our study, we demonstrate the value of orthogonally touching the endocardial surface during EAM for propagation wavefront- independent mapping. This can be achieved e.g. by using a long sheath, and looping the catheter within the RV to optimally reach the peritricuspid region (Fig. 2) or the RVOT using the reverse U-curve technique [34].

4.4. Limitations

This was a small single-center study and is limited by the low number of patients since ARVC is a rare disease and because the force-sensing ablation catheter is not regularly used to treat patients without structural heart disease. Moreover, since patients fulfilled a definite diagnosis of ARVC according to the 2010 TFC, this population does not represent the very early disease stages or left-dominant forms in which EAM may be particularly useful to establish a timely diagnosis. Lastly, since patients were mostly recruited without an indication for VT ablation, we did not perform epicardial mapping for the purpose of this study.

5. Conclusions

EAM using CFSC validates previous bipolar cut-off values for normal endocardial RV voltage amplitudes. RV voltages are generally lower in ARVC as compared to controls, with the subtricuspid area being commonly affected and having the highest discriminatory power to differentiate between ARVC and healthy controls. Therefore, EAM using CFSC constitutes a promising tool for diagnosis of ARVC.

Author contributions

Conceptualization: AMS, CBB, FD; Data curation: AMS; Formal analysis: VAR; Funding acquisition: AMS, CBB, FD; Investigation: DL, MM, DA, SC, AG; Methodology: AMS, CBB, FD; Project administration: AMS, VAR, DL; Supervision: AMS, CBB, SK; Validation: AMS, VAR; Visualization: AMS, DL, MM, DA, SC, AG, FD, CBB, VAR; Roles/Writing - original draft: VAR, DL; Writing - review & editing: AMS, VAR.

Declaration of Competing Interest

AMS received educational grants through his institution from Abbott, Bayer Healthcare, Biosense Webster, Biotronik, Boston Scientific, BMS/Pfizer, and Medtronic; and speaker /advisory board /consulting fees from Biotronik, Daichii-Sankyo, Medtronic, Novartis and StrideBio.

CBB received speaker /advisory board /consulting fees from Johnson&Johnson, Abbott, AstraZeneca, Novartis, and Pfizer.

Acknowledgements

The Zurich ARVC Program is supported by the Georg und Bertha Schwyzer-Winiker Foundation, Baugarten Foundation, Wild Foundation, Swiss National Science Foundation (SNF), and the Swiss Heart Foundation. We would like to thank Prof. Burkhardt Seifert, Institute for Social- and Preventive Medicine, University of Zürich, for expert statistical advice.

Values are median (25% and 75% interquartile range). Abbreviations: RV, right ventricular; RVOT, right ventricular outflow tract. *P values for comparisons between groups total were calculated using repeated measurements ANOVA, whereas single groups comparisons were performed with Mann-Whitney-U test.

Appendix A. Supplementary data

Supplementary data to this article can be found online at https://doi.org/10.1016/j.ijcard.2023.131289.

References

[1] A.M. Saguner, A. Medeiros-Domingo, M.A. Schwyzer, et al., Usefulness of inducible ventricular tachycardia to predict long-term adverse outcomes in arrhythmogenic right ventricular cardiomyopathy, Am. J. Cardiol. 111 (2) (2013) 250–257.
[2] A. Tabib, A. Miras, P. Taniere, R. Loire, Undetected cardiac lesions cause unexpected sudden cardiac death during occasional sport activity. A report of 80 cases, Eur. Heart J. 20 (12) (1999) 900–903.
[3] D. Corrado, P.J. van Tintelen, W.J. McKenna, et al., Arrhythmogenic right ventricular cardiomyopathy: evaluation of the current diagnostic criteria and differential diagnosis, Eur. Heart J. 41 (14) (2020) 1414–1429.
[4] N. Molitor, F. Duru, Arrhythmogenic right ventricular cardiomyopathy and differential diagnosis with diseases mimicking its phenotypes, J. Clin. Med. 11 (5) (2022).
[5] A. Gasperetti, V.A. Rossi, A. Chiodini, et al., Differentiating hereditary arrhythmogenic right ventricular cardiomyopathy from cardiac sarcoidosis fulfilling 2010 ARVC task force criteria, Heart Rhythm. 18 (2) (2021) 231–238.
[6] M. Boulos, I. Lashevsky, S. Reisner, L. Gepstein, Electroanatomic mapping of arrhythmogenic right ventricular dysplasia, J. Am. Coll. Cardiol. 38 (7) (2001) 2020–2027.
[7] M. Boulos, I. Lashevsky, L. Gepstein, Usefulness of electroanatomical mapping to differentiate between right ventricular outflow tract tachycardia and arrhythmogenic right ventricular dysplasia, Am. J. Cardiol. 95 (8) (2005) 935–940.
[8] M. Pieroni, A. Dello Russo, F. Marzo, et al., High prevalence of myocarditis mimicking arrhythmogenic right ventricular cardiomyopathy differential diagnosis by electroanatomic mapping-guided endomyocardial biopsy, J. Am. Coll. Cardiol. 53 (8) (2009) 681–689.
[9] D. Corrado, M. Perazzolo Marra, A. Zorzi, et al., Diagnosis of arrhythmogenic cardiomyopathy: the Padua criteria, Int. J. Cardiol. 319 (2020) 106–114.
[10] F.I. Marcus, W.J. McKenna, D. Sherrill, et al., Diagnosis of arrhythmogenic right ventricular cardiomyopathy/dysplasia: proposed modification of the task force criteria, Eur. Heart J. 31 (7) (2010) 806–814.
[11] T. Ustunkaya, B. Desjardins, R. Wedan, et al., Epicardial conduction speed, electrogram abnormality, and computed tomography attenuation associations in arrhythmogenic right ventricular cardiomyopathy, JACC Clin. Electrophysiol. 5 (10) (2019) 1158–1167.
[12] M. Kubala, S. Xie, P. Santangeli, et al., Analysis of local ventricular repolarization using unipolar recordings in patients with arrhythmogenic right ventricular cardiomyopathy, J. Interv. Card. Electrophysiol. 57 (2) (2020) 261–270.
[13] K. Zeppenfeld, P. Kies, M.C. Wijffels, M. Bootsma, L. van Erven, M.J. Schalij, Identification of successful catheter ablation sites in patients with ventricular tachycardia based on electrogram characteristics during sinus rhythm, Heart Rhythm. 2 (9) (2005) 940–950.
[14] H. Klein, R.B. Karp, N.T. Kouchoukos, G.L. Zorn Jr., T.N. James, A.L. Waldo, Intraoperative electrophysiologic mapping of the ventricles during sinus rhythm in patients with a previous myocardial infarction. Identification of the electrophysiologic substrate of ventricular arrhythmias, Circulation. 66 (4) (1982) 847–853.
[15] K.T. Konings, J.L. Smeets, O.C. Penn, H.J. Wellens, M.A. Allessie, Configuration of unipolar atrial electrograms during electrically induced atrial fibrillation in humans, Circulation. 95 (5) (1997) 1231–1241.
[16] M.D. Hutchinson, E.P. Gerstenfeld, B. Desjardins, et al., Endocardial unipolar voltage mapping to detect epicardial ventricular tachycardia substrate in patients with nonischemic left ventricular cardiomyopathy, Circ. Arrhythm. Electrophysiol. 4 (1) (2011) 49–55.
[17] S. Kirubakaran, C. Bisceglia, J. Silberbauer, et al., Characterization of the arrhythmogenic substrate in patients with arrhythmogenic right ventricular cardiomyopathy undergoing ventricular tachycardia ablation, Europace. 19 (6) (2017) 1049–1062.
[18] G. Breithardt, M.E. Cain, N. El-Sherif, et al., Standards for analysis of ventricular late potentials using high resolution or signal-averaged electrocardiography. A statement by a task force committee between the European Society of Cardiology, the American Heart Association and the American College of Cardiology, Eur. Heart J. 12 (4) (1991) 473–480.
[19] G.M. Polin, H. Haqqani, W. Tzou, et al., Endocardial unipolar voltage mapping to identify epicardial substrate in arrhythmogenic right ventricular cardiomyopathy/dysplasia, Heart Rhythm. 8 (1) (2011) 76–83.
[20] Z.H. Tseng, GEP. Outflow tract ven tricular tachyarrhythmias, in: Cardiac Electrophysiology: From Cell to Bedside, Seventh edition, 2018.
[21] F.E. Marchlinski, D.J. Callans, C.D. Gottlieb, E. Zado, Linear ablation lesions for control of unmappable ventricular tachycardia in patients with ischemic and nonischemic cardiomyopathy, Circulation. 101 (11) (2000) 1288–1296.
[22] D. Corrado, C. Basso, L. Leoni, et al., Three-dimensional electroanatomic voltage mapping increases accuracy of diagnosing arrhythmogenic right ventricular cardiomyopathy/dysplasia, Circulation. 111 (23) (2005) 3042–3050.
[23] T.P. Mast, K. Taha, M.J. Cramer, et al., The prognostic value of right ventricular deformation imaging in early arrhythmogenic right ventricular cardiomyopathy, JACC Cardiovasc. Imaging 12 (3) (2019) 446–455.
[24] C. Basso, F. Ronco, F. Marcus, et al., Quantitative assessment of endomyocardial biopsy in arrhythmogenic right ventricular cardiomyopathy/dysplasia: an in vitro validation of diagnostic criteria, Eur. Heart J. 29 (22) (2008) 2760–2771.
[25] M. Masjedi, C. Jungen, P. Kuklik, et al., A novel algorithm for 3-D visualization of electrogram duration for substrate-mapping in patients with ischemic heart disease and ventricular tachycardia, PLoS One 16 (7) (2021), e0254683.
[26] V.A. Rossi, D. Niederseer, J.M. Sokolska, et al., A novel diagnostic score integrating atrial dimensions to differentiate between the Athlete's heart and arrhythmogenic right ventricular cardiomyopathy, J. Clin. Med. 10 (18) (2021).
[27] D. Niederseer, V.A. Rossi, C. Kissel, et al., Role of echocardiography in screening and evaluation of athletes, Heart. (2020 Nov 17), heartjnl-2020-317996, https://doi.org/10.1136/heartjnl-2020-317996.
[28] S. Mathew, A.M. Saguner, N. Schenker, et al., Catheter ablation of ventricular tachycardia in patients with Arrhythmogenic right ventricular cardiomyopathy/dysplasia: a sequential approach, J. Am. Heart Assoc. 8 (5) (2019), e010365.
[29] A.S. Te Riele, C.A. James, B. Philips, et al., Mutation-positive arrhythmogenic right ventricular dysplasia/cardiomyopathy: the triangle of dysplasia displaced, J. Cardiovasc. Electrophysiol. 24 (12) (2013) 1311–1320.
[30] J.C. Hoogendoorn, M. Sramko, J. Venlet, et al., Electroanatomical voltage mapping to distinguish right-sided cardiac sarcoidosis from arrhythmogenic right ventricular cardiomyopathy, JACC Clin. Electrophysiol. 6 (6) (2020) 696–707.
[31] M. Casella, F. Perna, A. Dello Russo, et al., Right ventricular substrate mapping using the Ensite Navx system: accuracy of high-density voltage map obtained by automatic point acquisition during geometry reconstruction, Heart Rhythm. 6 (11) (2009) 1598–1605.

[32] M. Hwang, J. Kim, B. Lim, et al., Multiple factors influence the morphology of the bipolar electrogram: an in silico modeling study, PLoS Comput. Biol. 15 (4) (2019), e1006765.
[33] M.W. Keller, S. Schuler, A. Luik, et al., Comparison of simulated and clinical intracardiac electrograms, Annu. Int. Conf. IEEE Eng. Med. Biol. Soc. 2013 (2013) 6858–6861.
[34] Z. Liao, X. Zhan, S. Wu, et al., Idiopathic ventricular arrhythmias originating from the pulmonary sinus cusp: prevalence, electrocardiographic/electrophysiological characteristics, and catheter ablation, J. Am. Coll. Cardiol. 66 (23) (2015) 2633–2644.